Canadian Journal of Cardiology 40 (2024) 372–384

Clinical Research

Characteristics and Clinical Value of Electroanatomic Voltage Mapping in Cardiac Amyloidosis

Michela Casella, MD, PhD,[a,b,‡] Paolo Compagnucci, MD, PhD,[a,‡] Giuseppe Ciliberti, MD, PhD,[a] Umberto Falanga, MD,[a,c] Alessandro Barbarossa, MD,[a] Yari Valeri, MD,[a,c] Laura Cipolletta, MD, PhD,[a] Giovanni Volpato, MD,[a,c] Giulia Stronati, MD,[a,c] Stefania Rizzo, MD,[d] Monica De Gaspari, MD,[d] Fabio Vagnarelli, MD, PhD,[e] Carla Lofiego, MD, PhD,[e] Gian Piero Perna, MD,[e] Andrea Giovagnoni, MD, PhD,[b] Andrea Natale, MD, FHRS,[f] Cristina Basso, MD, PhD,[d] Federico Guerra, MD,[a,c] and Antonio Dello Russo, MD, PhD[a,c]

[a] *Cardiology and Arrhythmology Clinic, University Hospital "Azienda Ospedaliero–Universitaria delle Marche," Ancona, Italy*

[b] *Department of Clinical, Special, and Dental Sciences, Marche Polytechnic University, Ancona, Italy*

[c] *Department of Biomedical Sciences and Public Health, Marche Polytechnic University, Ancona, Italy*

[d] *Cardiovascular Pathology Unit, Department of Cardiac, Thoracic, Vascular Sciences, and Public Health, Azienda Ospedaliera–University of Padua, Padova, Italy*

[e] *Division of Cardiology, University Hospital "Azienda Ospedaliero–Universitaria delle Marche," Ancona, Italy*

[f] *Texas Cardiac Arrhythmia Institute, Austin, Texas, USA*

See editorial by Nery and Birnie, pages 385-387 of this issue.

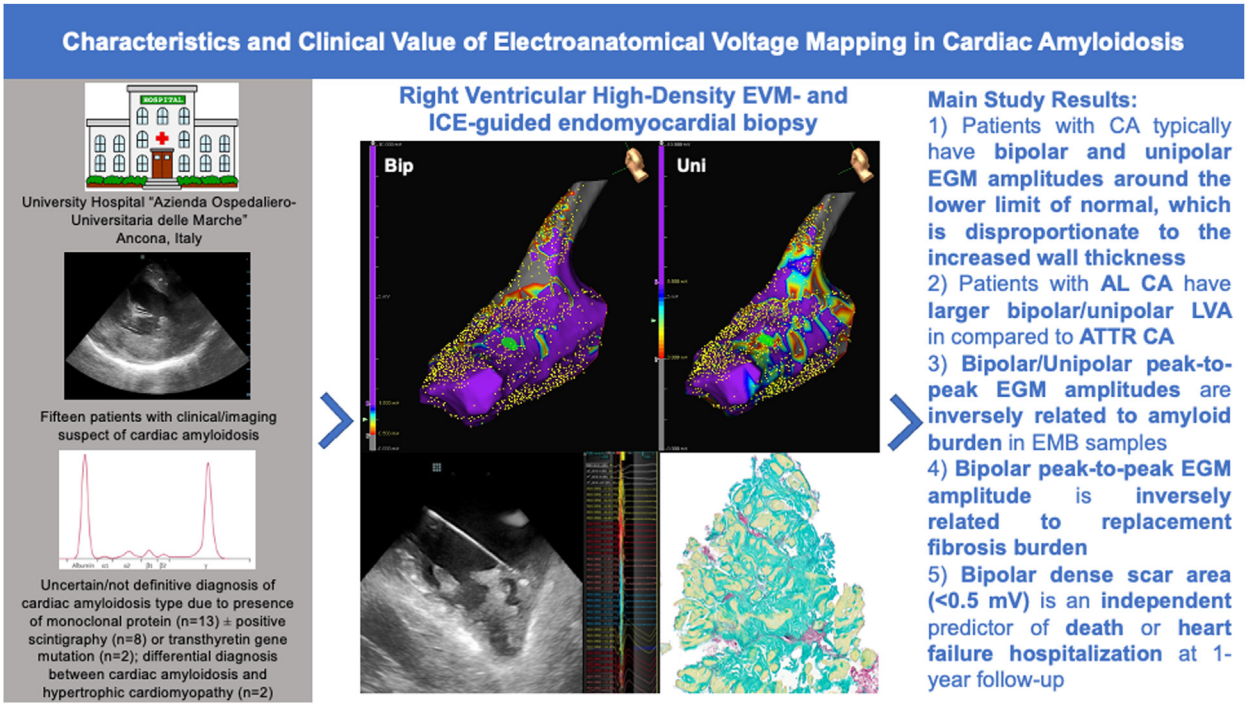

https://doi.org/10.1016/j.cjca.2023.10.022

ABSTRACT

Background: Cardiac amyloidoses (CAs) are an increasingly recognised group of infiltrative cardiomyopathies associated with high risk of adverse cardiac events. We sought to characterise the characteristics and clinical value of right ventricular (RV) electroanatomic voltage mapping (EVM) in CA.

Methods: Fifteen consecutive patients undergoing endomyocardial biopsy (EMB) for suspected CA (median age 75 years, 1st-3rd quartiles 64-78 years], 67% male) were enrolled in an observational prospective study. Each patient underwent RV high-density EVM using a multipolar catheter and EMB. The primary outcome was death or heart failure hospitalisation at 1-year follow-up. We recorded electrographic features at EMB sampling sites and electroanatomic data in the overall RV, and explored their correlations with histopathologic findings and primary outcomes events.

Results: A final EMB-proven diagnosis of immunoglobulin light chain or transthyretin CA was formulated in 6 and 9 patients, respectively. Electrogram amplitudes in the bipolar and unipolar configurations averaged 1.55 $\pm$ 0.44 mV and 5.14 $\pm$ 1.50 mV, respectively, in the overall RV, with lower values in AL CA patients. We found a significant inverse correlation between both bipolar and unipolar electrogram amplitude and amyloid burden according to EMB ($P = 0.001$ and $P = 0.025$, respectively). At 1-year follow-up, 7 patients (47%) experienced a primary outcome event; the extent of bipolar dense scar area at RV EVM was an independent predictor of primary outcome events at multivariable analysis (odds ratio 2.40; $P = 0.037$).

Conclusions: In CA, electrogram amplitudes are around the lower limit of normal yet disproportionately low compared with the increased wall thickness. Out data suggest that RV electrogram amplitude may be a quantitative marker of amyloid burden, and that RV EVM may have prognostic value.

RÉSUMÉ

Contexte : Les amyloïdoses cardiaques constituent un groupe de plus en plus reconnu de cardiomyopathies infiltrantes associées à un risque élevé d'événements cardiaques. Nous souhaitions définir les caractéristiques et la valeur clinique de la cartographie électro-anatomique ventriculaire droite dans l'amyloïdose cardiaque.

Méthodologie : Quinze patients consécutifs subissant une biopsie endomyocardique pour une amyloïdose cardiaque suspectée (âge médian de 75 ans, 1er-3^{e} quartiles 64-78 ans, 67 % hommes) ont été recrutés dans une étude prospective observationnelle. Chaque patient a été soumis à une cartographie électro-anatomique de haute densité du ventricule droit au moyen d'un cathéter multipolaire et d'une biopsie endomyocardique. Le principal critère d'évaluation était le décès ou une hospitalisation pour insuffisance cardiaque après un suivi de 1 an. Nous avons consigné les caractéristiques électrographiques aux points de prélèvement des échantillons endomyocardiques et les données électro-anatomiques de l'ensemble du ventricule droit et nous avons étudié leurs corrélations avec des observations histopathologiques et des événements liés aux critères d'évaluation principaux.

Résultats : Un diagnostic final, confirmé par biopsie endomyocardique, d'amyloïdose cardiaque à chaînes légères d'immunoglobuline ou à transthyrétine a été établi chez respectivement 6 et 9 patients. Les amplitudes de l'électrogramme dans les configurations bipolaire et unipolaire étaient en moyenne respectivement de 1,55 $\pm$ 0,44 mV et de 5,14 $\pm$ 1,50 mV dans l'ensemble du ventricule droit, les valeurs inférieures étant observées chez les patients atteints d'amyloïdose cardiaque à chaînes légères d'immunoglobuline. Nous avons trouvé une corrélation négative importante entre l'amplitude de l'électrogramme bipolaire et unipolaire et la charge amyloïde sur la base de la biopsie endomyocardique ($p = 0,001$ et $p = 0,025$, respectivement). Après 1 an de suivi, 7 patients (47 %) avaient présenté un épisode lié au critère d'évaluation principal; l'étendue de la zone de lésions dense bipolaire à la cartographie électro-anatomique ventriculaire droite constituait un facteur prédictif indépendant pour les épisodes liés au critère d'évaluation principal dans l'analyse multivariable (risque relatif approché 2,40; $p = 0,037$).

Conclusions : Dans l'amyloïdose cardiaque, les amplitudes à l'électrogramme se situent près de la limite inférieure de la normale, bien que proportionnellement très faible par rapport à l'épaisseur accrue de la paroi. Des données laissent croire que l'amplitude de l'électrogramme ventriculaire droit peut être un marqueur quantitatif de la charge amyloïde et que la cartographie électro-anatomique du ventricule droit peut avoir une valeur pronostique.

Cardiac amyloidoses (CAs) are an increasingly recognised group of infiltrative cardiomyopathies associated with high risk of heart failure, thromboembolic events, and arrhythmias.[1-3] Although several types of CA may be distinguished according to the amyloid precursor protein, immunoglobulin light chain (AL) and transthyretin (ATTR) CAs account for > 98% of currently diagnosed cases.[1]

During recent years, the introduction into clinical practice of specific and effective therapies for ATTR CA has prompted an increasing interest in the noninvasive diagnosis of this type of CA[4] by means of nuclear medicine and laboratory tests.[1] Nonetheless, endomyocardial biopsy (EMB) remains the criterion standard for diagnosis of CA as well as for the classification of the amyloid fibril protein and is indicated in several clinical scenarios.[1-8] Previous work showed that electroanatomic voltage mapping (EVM) increases diagnostic yield of EMB in cardiomyopathies with focal myocardial involvement[9-13] and that it may provide prognostic information.[14] As of today, electroanatomic features of CA have not

Received for publication July 21, 2023. Accepted October 26, 2023.

‡These authors contributed equally to this work.

Corresponding author: Dr Paolo Compagnucci, Cardiology and Arrhythmology Clinic, Marche University Hospital, Via Conca 71, 60126, Ancona, Italy. Tel.: +390715965210; fax: +390715963041.
E-mail: paolocompagnucci1@gmail.com
Twitter: @CompagnucciMD

See page 383 for disclosure information.

been reported, and whether EVM may have prognostic value in this clinical setting is unclear.

In the present study, we assessed whether electrographic/electroanatomic features are related to EMB findings and clinical outcomes in a cohort of patients undergoing right ventricular (RV) high-density EVM and EMB for suspected CA.

Methods

Study population

We conducted an observational, prospective, single-centre study including all consecutive patients with suspected CA undergoing RV EVM and EMB at a referral centre (University Hospital "Azienda Ospedaliero-Universitaria delle Marche," Ancona, Italy) from December 2019 to July 2022. For each patient, we collected demographics, clinical information, procedural details, and follow-up data. The study was performed according to institutional standards, national legal requirements, and the Declaration of Helsinki, and the study protocol was approved by the Institutional Review Board. The authors confirm that patient consent forms were obtained for this article. The data that support the findings of this study are available from the corresponding author by reasonable request.

Clinical and imaging assessments

Twelve-lead electrocardiography (ECG) and transthoracic echocardiography were performed for all patients during their hospitalisations for EVM and EMB, and hydroxydiphosphonate technetium (^{99m}Tc-HDP) scintigraphy was performed within 6 months of EVM and EMB in all patients, and classified according to a previously reported grading system.[1,15] Clonal dyscrasia was excluded within 6 months of the invasive procedure; the use of cardiac magnetic resonance imaging (CMR) was at the discretion of the treating physicians. All patients with a strong clinical suspicion of ATTR CA underwent genetic testing for transthyretin (TTR) mutations to differentiate between hereditary and acquired ATTR CA.[1] Detailed methods for the clinical and imaging assessments are described in Supplemental Appendix S1.

Indications for EMB

In all patients enrolled in this study, 4 main clinical scenarios prompted EMB, in accordance with international recommendations[1]: 1) coexistence of monoclonal protein and grade 2/3 ^{99m}Tc-HDP scintigraphy (n = 8); 2) evidence of monoclonal protein, imaging findings supporting CA, and grade 0 ^{99m}Tc-HDP scintigraphy (n = 4); 3) doubtful differential diagnosis with hypertrophic cardiomyopathy (n = 2, one of whom had undergone septal myectomy for suspected hypertrophic obstructive cardiomyopathy in the past but had imaging suspicion of CA and evidence of TTR gene mutation); and 4) coexistence of monoclonal protein and TTR gene mutation (n = 1).

High-density EVM and intracardiac echocardiography

EVM was performed during the same procedure as and immediately before EMB, during sinus rhythm, in the conscious and fasting state, using the EnSite Precision cardiac mapping system (Abbott, Plymouth, MN). High-density voltage maps of the RV were reconstructed with the use of the paddle-shaped Advisor HD Grid Mapping Catheter Sensor Enabled (Abbott) (Supplemental Appendix S1). Intracardiac echocardiography (ICE) also was performed during the procedure, using the ViewFlex probe (Abbott), to ensure adequate catheter-tissue contact, as well as to monitor for intraprocedural complications.[16] Points generated by adequate catheter-tissue contact as assessed by ICE and fluoroscopy, with stable cycle length, local activation time, and voltage amplitude during 3 consecutive beats, were acquired and used for the reconstruction of RV unipolar and bipolar (using the HD-wave solution; see Supplemental Appendix S1 for details) EVM. Throughout the study, low voltage was defined based on standard peak-to-peak voltage criteria (low-voltage areas [LVAs]: $\leq$ 1.5 mV for bipolar electrogram [EGM] peak-to-peak amplitude [BV] and $\leq$ 5.5 mV for unipolar EGM peak-to-peak amplitude [UV]; bipolar dense scar area [DSA]: $<$ 0.5 mV).[9] After EGM analysis, the extents of endocardial LVAs in bipolar and unipolar EVMs were measured as both absolute values (cm^2) and relative values (percentage of all RV mapped area). We also recorded the locations of endocardial LVAs, by dividing the RV into 4 regions, as previously described[17]: interventricular septum, RV outflow tract, subtricuspid RV (including anterior and posterior RV free wall), and apex. The BVs and UVs of all acquired mapping points were exported from the electroanatomic mapping system into data files, and bipolar and unipolar durations and numbers of peaks at EMB sampling sites (see the following sections on EMB) also were recorded. Furthermore, any presence of late potentials (defined as those EGMs with a component recorded after the inscription of the latest surface QRS activity) was noted.[13] Finally, the His bundle and right bundle branch electrograms were tagged in the EVM, and AH and HV intervals were measured, as previously described.[18] Programmed ventricular stimulation (PVS) was performed at operators' discretion (Supplemental Appendix S1).[19]

EMB

RV EMB samples were obtained with the use of a disposable bioptome (Cordis, Johnson, and Johnson, Bridgewater, NJ) introduced into a steerable sheath (Agilis NxT; Abbott) from the right femoral venous access.[10] Because CA is a diffuse infiltrative disease process, the interventricular septum was chosen as the preferred target region for EMB. Once the target area was chosen according to the ease of reach within the interventricular septum, the bioptome was connected to the electroanatomic mapping system to allow visualisation of the bioptome and tagging of the EMB sampling site in the EVM, as previously described.[10] Briefly, a small screw was inserted into the adapter of the bioptome handle, allowing connection of 2 alligator clips to the bioptome catheter; the electric cables were then connected to the EnSite Precision mapping system.[10] As an additional advantage of this technique, the visualisation of the bioptome in the EVM allowed us to avoid injuring the atrioventricular conduction system, which is commonly abnormal in CA.[3,18] A minimum of 3 samples were obtained per patient. All EMB samples were referred to the Cardiovascular Pathology Unit at the University Hospital in Padua. The EMBs were fixed in 10% buffered formalin (pH 7.35) and processed for histologic examination.

Table 1. Baseline clinical, electrocardiographic, and imaging characteristics of patients according to the type of cardiac amyloidosis (AL vs ATTR)

	Overall (n = 15)	AL CA (n = 6)	ATTR CA (n = 9)	*P* value
Age, y	75 (64-78)	64 (53-66)	77 (76-78)	0.008*
Female sex	5 (33)	3 (50)	2 (22)	0.329
NYHA functional class				
II	6 (40)	3 (50)	3 (33)	0.622
III	9 (60	3 (50)	6 (67)	0.622
BMI, kg/m^2	24.9 ± 3.6	24.5 ± 3.9	25.3 ± 3.6	0.691
COPD	3 (20)	1 (17)	2 (11)	1.000
TTR variant	2 (13)	1 (10)	1 (0)	1.000
CIED carrier	0 (0)	0 (0)	0 (0)	1.000
^{99m}Tc-HDP scintigraphy grading				
0	5 (33)	5 (83)	0 (0)	0.002*
2	7 (47)	1 (17)	6 (66)	0.119
3	3 (20)	0 (0)	3 (33)	0.229
Time interval between ^{99m}Tc-HDP scintigraphy and endomyocardial biopsy, d	150 (74-160)	58 (20-130)	150 (140-160)	0.076
GFR, mL/min	75 ± 21	83 ± 25	69 ± 17	0.258
NT-proBNP, ng/L	1929 (876-4901)	4804 (2294-4998)	1236 (622-1815)	0.178
Disease stage	2 (1-3)	3 (2-3)	1 (1-2)	0.027*
History of atrial fibrillation	8 (53)	2 (33)	6 (67)	0.315
Nonsustained ventricular tachycardia	4 (27)	3 (50)	1 (11)	0.235
Electrocardiographic data				
Low QRS voltage	11 (73)	5 (83)	6 (66)	0.604
Limb QRS score, mV	22 ± 6	18 ± 6	25 ± 5	0.057
Precordial QRS score, mV	55 ± 16	41 ± 7	65 ± 14	< 0.001*
Total QRS score, mV	77 ± 21	59 ± 10	86 ± 17	0.001*
Atrial fibrillation	4 (27)	0 (0)	4 (44)	0.103
PR interval, ms	189 ± 38	184 ± 52	194 ± 17	0.670
Any intraventricular conduction disturbance	9 (60)	4 (67)	5 (56)	1.000
LBBB	3 (20)	1 (17)	2 (22)	1.000
RBBB	2 (13)	1 (17)	1 (11)	1.000
LAFB	2 (13)	2 (33)	1 (11)	0.525
LPFB	2 (13)	1 (17)	1 (11)	1.000
T-wave inversion	6 (40)	4 (67)	2 (22)	0.136
Imaging data†				
Maximal septal thickness, mm	18 (17-19)	17 (16-18)	19 (18-20)	0.014*
Posterior wall thickness, mm	16 ± 2	16 ± 2	16 ± 3	0.477
LVEDD, mm	40 ± 5	39 ± 3	41 ± 6	0.278
iLVEDV, mL/m^2	47 ± 9	45 ± 12	48 ± 8	0.605
iLAV, mL/m^2	45 (39-49)	41 (38-45)	48 (40-51)	0.125
LVEF, %	51 ± 13	46 ± 16	54 ± 10	0.281
E/e′ ratio	19 ± 6	23 ± 5	16 ± 5	0.046*
RVD1, mm	35 ± 5	34 ± 6	36 ± 4	0.422
Right atrial area, cm^2	20 ± 7	18 ± 5	20 ± 9	0.603
TAPSE, mm	17 ± 3	17 ± 2	18 ± 4	0.598
sPAP, mm Hg	30 (28-50)	30 (29-40)	40 (27-52)	0.768
RV hypertrophy	15 (100)	6 (100)	9 (100)	1.000
RV free wall thickness, mm	8 ± 1	8 ± 1	8 ± 1	0.616
CMR performed	7 (47)	5 (83)	2 (22)	0.041*
LGE	7 (100)	5 (100)	2 (100)	1.000
RV LGE	7 (100)	5 (100)	2 (100)	1.000
Diffuse LGE	7 (100)	5 (100)	2 (100)	1.000
Medical treatments				
Tafamidis	7 (47)	0 (0)	7 (78)	0.007*
Loop diuretics	12 (80)	6 (100)	6 (67)	0.229
Mineralocorticoid receptor antagonists	7 (47)	3 (50)	4 (44)	1.000
Thiazide/thiazide-like diuretics	1 (7)	0 (0)	1 (11)	1.000
SGLT2 inhibitors	1 (7)	0 (0)	1 (11)	1.000
Oral anticoagulants	6 (40)	1 (17)	5 (56)	0.287
Antiplatelets	4 (27)	1 (17)	3 (33)	0.604
Statins	10 (67)	3 (50)	7 (78)	0.329
Beta-blockers	6 (40)	0 (0)	6 (67)	0.028*
Amiodarone	1 (7)	0 (0)	1 (11)	1.000
Angiotensin-converting enzyme inhibitors	2 (13)	0 (0)	2 (22)	0.486
Angiotensin receptor blockers	2 (13)	0 (0)	2 (22)	0.486

Values are presented as median (1st-3rd quartiles), n (%), or mean ± SD.

AL, immunoglobulin light chain—related; ATTR, transthyretin-related; BMI, body mass index; CIED, cardiac implantable electronic device; CMR, cardiac magnetic resonance imaging; COPD, chronic obstructive pulmonary disease; GFR, glomerular filtration rate; iLAV, indexed left atrial volume; iLVEDV, indexed left ventricular end-diastolic volume; LAFB, left anterior fascicular block; LBBB, left bundle branch block; LGE, late gadolinium enhancement; LPFB, left posterior fascicular block; LVEDD, left ventricular end-diastolic diameter; LVEF, left ventricular ejection fraction; NT-proBNP, N-terminal pro—B-type natriuretic peptide; NYHA, New York Heart Association; RBBB, right bundle branch block; RV, right ventricular; RVD1, basal right ventricular diameter; SGLT2, sodium-glucose cotransporter 2; sPAP, systolic pulmonary artery pressure; TAPSE, tricuspid annular plane systolic excursion; ^{99m}Tc-HDP, hydroxydiphosphonate technetium; TTR, transthyretin.

* $P < 0.05$.

† For wall thickness, volumes, and ejection fractions, cardiac magnetic resonance data were reported when available.

Table 2. Electroanatomic and histopathologic characteristics according to the type of CA

	Overall (n = 15)	AL CA (n = 6)	ATTR CA (n = 9)	*P* value
Electrophysiologic/electroanatomic data				
Procedural duration, min	79 ± 22	93 ± 22	70 ± 19	0.073
AH interval, ms	124 ± 33	117 ± 42	132 ± 18	0.454
HV interval, ms	60 ± 12	68 ± 13	55 ± 9	0.072
PVS performed	3 (20)	2 (33)	1 (11)	0.525
Sustained VA induction at PVS	0 (0)	0 (0)	0 (0)	1.000
No. of mapped points	2552 (1855-8836)	5435 (2342-8282)	2533 (1640-9201)	0.689
RV mapped area, cm^2	183 ± 29	180 ± 33	185 ± 27	0.741
Bipolar low-voltage zone (< 1.5 mV)				
Absolute value, cm^2	12.1 ± 8.2	18.0 ± 5.5	8.2 ± 7.5	0.012*
Percentage	7 (2-10)	10 (9-11)	2 (2-6)	0.012*
Bipolar dense scar (< 0.5 mV)				
Absolute value, cm^2	3.0 (1.7-5.2)	5.8 (3.2-8.0)	2.0 (1.1-3.2)	0.044*
Percentage value	2 ± 1	3 ± 1	1 ± 1	0.018*
Unipolar low-voltage zone (< 5.5 mV, cm^2)				
Absolute value, cm^2	20.4 ± 13.0	32.3 ± 6.1	12.4 ± 9.6	< 0.001*
Percentage	11 ± 7	18 ± 3	7 ± 5	< 0.001*
Regional distribution of low-voltage zones				
Unipolar map				
Interventricular septum	9 (60)	6 (100)	3 (33)	0.028*
RV outflow tract	14 (93)	6 (100)	8 (89)	1.000
Subtricuspid RV	10 (66)	5 (83)	5 (56)	0.580
RV apex	4 (27)	3 (50)	1 (11)	0.235
Bipolar map				
Interventricular septum	11 (73)	6 (100)	5 (56)	0.103
RV outflow tract	14 (93)	5 (83)	9 (100)	0.400
Subtricuspid RV	12 (80)	5 (83)	7 (78)	1.000
RV apex	5 (33)	1 (17)	4 (44)	0.580
EMB data				
Total no. of samples	57 (100)	24 (42)	33 (58)	0.134
Site of sampling				
Interventricular septum	57 (100)	24 (42)	33 (58)	0.134
Amyloid percentage	22 (9-36)	25 (9-34)	17 (9-36)	0.797
Replacement-type fibrosis percentage	2 (0-3)	0 (0-3)	3 (0-3)	0.129
Myocyte percentage	80 (63-92)	81 (68-92)	80 (62-91)	0.497
EGM characteristics at EMB sampling sites				
Bipolar EGM amplitude at sampling site, mV	2.3 (1.7-4.1)	2.3 (1.5-3.4)	2.4 (1.7-4.4)	0.374
Unipolar EGM amplitude at sampling site, mV	7.4 ± 2.5	6.9 ± 2.0	7.7 ± 2.8	0.212
Bipolar EGM duration at sampling site, msec	55 (44-64)	54 (44-61)	56 (45-65)	0.390
No. of EGM peaks at sampling site	2 (2-2)	2 (2-2)	2 (2-3)	0.230
Late potentials	0 (0)	0 (0)	0 (0)	1.000

Values are presented as mean ± SD, n (%), or median (1st-3rd quartiles).

AL, immunoglobulin light chain–related; ATTR, transthyretin-related; CA, cardiac amyloidosis; EGM, electrogram; EMB, endomyocardial biopsy; PVS, programmed ventricular stimulation; RV, right ventricular; VA, ventricular arrhythmia.

* $P < 0.05$.

The paraffin-included sections (5 μm thick) underwent serial cuts and staining with hematoxylin-eosin and Heidenhain trichrome. In addition, Congo red (with dedicated sections cut at 10 μm) and Sulfate Alcian Blue (SAB) stainings were performed to detect the presence of amyloid deposits.[5] SAB allows distinguishing of amyloid deposits (which are coloured in green) from replacement-type fibrosis (coloured in red) and cardiomyocytes (coloured in yellow).

EMB morphometric analysis

EMB specimens underwent detailed histopathologic analysis to assess the following data.

1) Amyloid burden: The amyloid area was calculated with a quantitative score on digitally acquired slides by means of an image analyser system and a commercially available software (Image-Pro Plus Version 4.0; Media Cybernetics, Rockville, MD). The analysis was performed on SAB-stained slides, and the result was expressed as the percentage of amyloid on each fragment for every patient.
2) Replacement-type fibrosis: The area of replacement-type fibrosis was calculated with a quantitative score on digitally acquired slides with the use of an image analyser system by the method described above on trichrome-stained slides, with the result expressed as the percentage of fibrosis on each fragment for every patient.

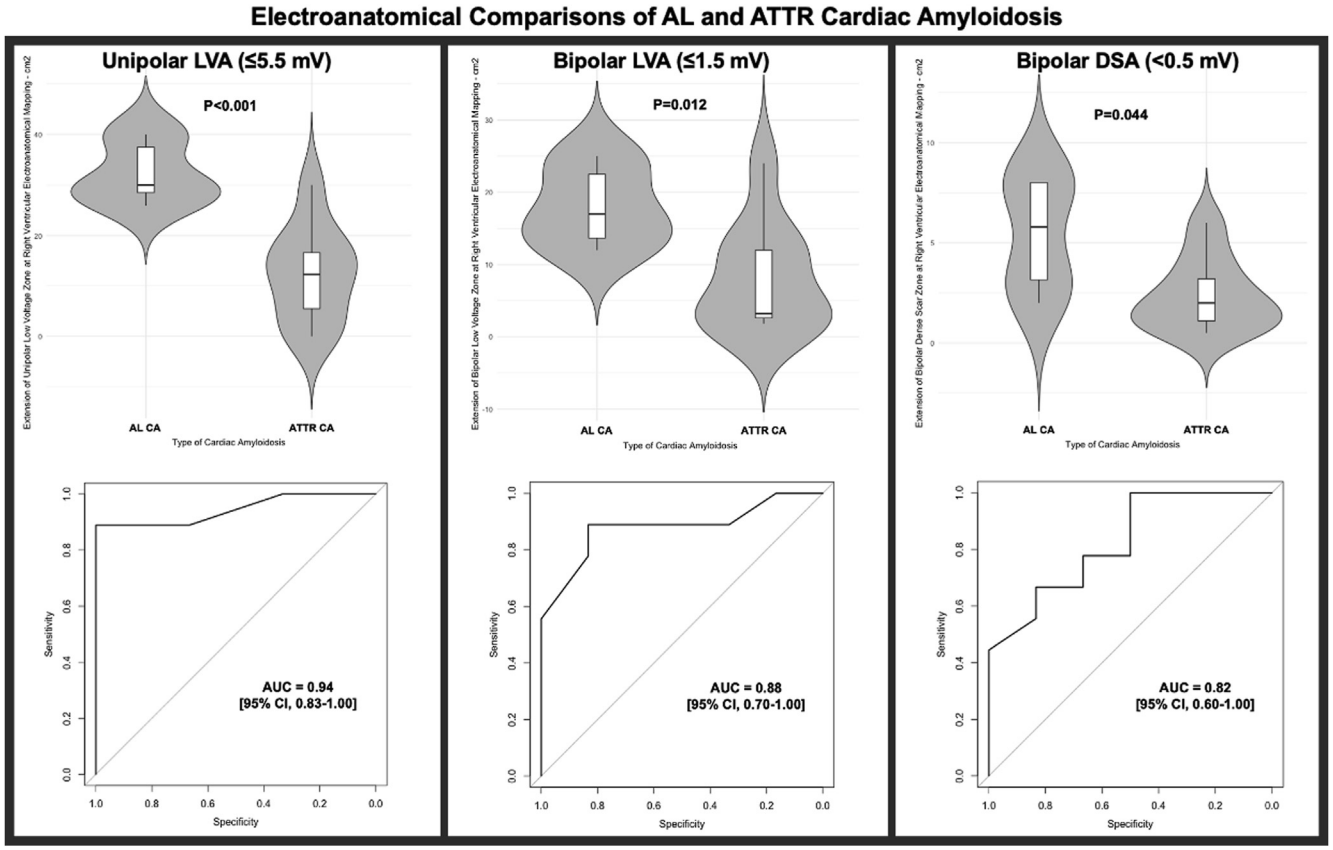

Figure 1. Electroanatomic comparisons between immunoglobulin light chain (AL)– and transthyretin (ATTR)–related cardiac amyloidoses (CAs). AUC, area under the receiver operatic characteristic curve; CI, confidence interval; DSA, dense scar area; LVA, low-voltage area.

Two cardiovascular pathologists, blinded to the patients' clinical data, performed the histopathologic analysis.

Amyloid typing with immune electron microscopy

Amyloid typing was performed with the use of immune electron microscopy on formalin-fixed paraffin-embedded blocks after dewaxing and resin embedding. Selected sections were then processed for postembedding immunogold. The primary antibodies used were anti–human kappa light chains, anti–human lambda light chains, and anti–human TTR.

Outcomes

The primary study outcome was a composite of death for cardiovascular causes and hospitalisation for heart failure worsening by 1 year of follow-up. Patients were systematically followed with clinic appointments at 3, 6, and 12 months after hospitalisation for the invasive procedure, and information concerning clinical events was collected.

Statistical analysis

Categoric data were expressed as absolute and relative frequencies, and compared by means of chi-square or Fisher exact test as appropriate. Continuous variables were checked for normality by means of the Shapiro-Wilk test and reported as mean and standard deviation if normally distributed, or median and 1st-3rd quartiles (Q1-Q3) if not normally distributed. Continuous variables were compared by means of Student t or Wilcoxon test, as appropriate. The correlation of EGM features at EMB sampling sites with EMB-proven amyloid or replacement-type fibrosis burdens were explored with the use of scatter plots and assessed with the use of linear regression models by clustering data from all patients. We determined the optimal EGM amplitude cutoffs associated with $>$ 15% amyloid burden at EMB with the use of the Youden index (the 15% threshold was chosen for being the median value in a recently proposed semiquantitative histopathologic score).[7] The association of LVA/DSA extent with CA type or primary outcome events was assessed by means of receiver operating characteristic curve analysis, and optimal cutoffs were determined with the use of the Youden index. Furthermore, the association of clinical, imaging, and electroanatomic variables with primary outcome events was assessed by means of logistic regression analysis; those variables with a P value < 0.05 in univariable analysis were entered into a multivariable model. Owing to a low event per variable ratio, the logistic regression model was penalized with the use of Firth's bias correction.[20] Furthermore, as a sensitivity analysis, the associations of pooled EGM amplitudes with biopsy-proven amyloid type and clinical outcomes were assessed by means of receiver operating characteristic curve analysis. A P value < 0.05 was considered to be statistically significant. All statistical analyses were performed with R software version 4.2.0 (R Foundation for Statistical Computing, Vienna, Austria).

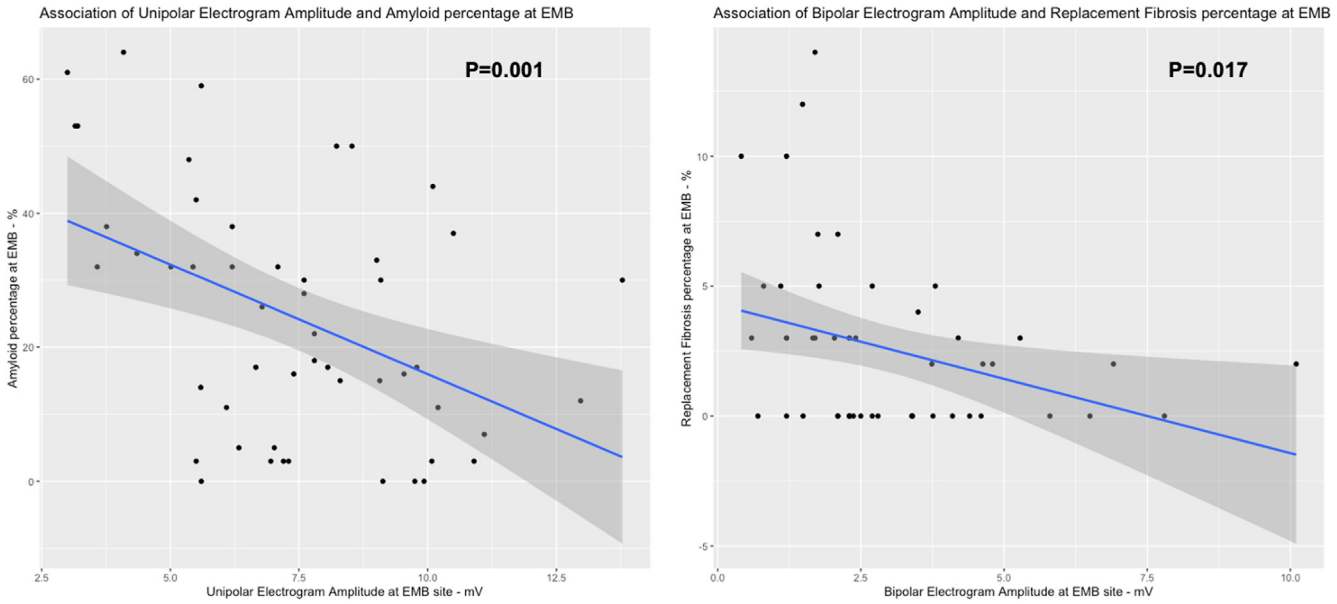

Figure 2. Scatter plots of the associations of (**left**) peak-to-peak unipolar electrogram amplitude with biopsy-proven amyloid burden and (**right**) peak-to-peak bipolar electrogram amplitude with biopsy-proven fibrosis burden at endomyocardial biopsy (EMB) sites.

Results

Study population and ECG, laboratory, and imaging findings

A total of 15 patients (median age 75 years, Q1-Q3 64-78 years, 10 (67%) male) underwent EVM and EMB for a clinical suspicion of CA and were enrolled in the study. The main demographic, clinical, laboratory, ECG, and imaging findings, both in the overall cohort and according to the EMB-proven type of CA are reported in Table 1.

All enrolled patients were evaluated because of symptomatic heart failure (New York Heart Association [NYHA] functional class II: n = 6 [40%]; NYHA functional class III: n = 9 [60%]), with significant elevation of N-terminal pro–B-type natriuretic peptide (NT-proBNP) levels, consistent with an advanced CA stage (median stage according to the Mayo staging systems: 2 [Q1-Q3 1-3]) (Supplemental Appendix S1) History of atrial fibrillation was common (n = 8; 53%). Remarkably, low QRS voltages and intraventricular conduction disturbances were evident in 11 (73%) and 9 (60%) patients, respectively, and symmetric concentric left ventricular hypertrophy was ubiquitously present, with median interventricular septal thickness of 18 mm. Thirteen subjects (87%) had laboratory evidence of monoclonal protein: multiple myeloma (MM) was diagnosed in 4 patients (IgG lambda in all cases), 8 patients had monoclonal gammopathy of unknown significance (MGUS), and 1 patient had a history of marginal zone lymphoma plus monoclonal protein. Gadolinium-enhanced CMR was performed in 7 patients (47%), demonstrating biventricular diffuse late gadolinium enhancement, highly suggestive of CA, in each case. Baseline 24-hour Holter monitoring was available in 5 patients (33%), and 6 subjects (40%) underwent 24-hour Holter monitoring during follow-up; sustained ventricular tachycardia was never recorded, whereas nonsustained ventricular tachycardia was recorded in 4 patients (2 at baseline monitoring, 1 during index hospitalisation, and 1 at follow-up monitoring) (Table 1).

In the comparison between AL and ATTR CAs, patients in the former group were younger, had lower precordial and total ECG QRS scores, lower interventricular septal thickness, and higher E/e′ ratio (Table 1).

EVM

Procedural, EVM, and EMB data are reported in Table 2, both in the overall study population and according to CA type. PVS was performed in 3 patients (20%) (2 with nonsustained ventricular tachycardia at Holter monitoring and 1 with doubtful differential diagnosis with hypertrophic cardiomyopathy), but sustained ventricular arrhythmias were never induced (Tables 2 and 4; Supplemental Table S1). Of note, high-density EVM of the RV were reconstructed, with a median number of 2552 acquired points per patient.

Peak-to-peak EGM amplitudes were around the lower limit of the normal range, with mean bipolar voltage amplitude of 1.55 ± 0.44 mV and mean unipolar voltage amplitude of 5.14 ± 1.50 mV. With the use of conventional unipolar and bipolar low voltage cutoffs, small LVAs could be demonstrated in each patient, involving 2 or more anatomic regions in 13 (87%) and 12 (80%) patients in bipolar and unipolar maps, respectively, with preeminent involvement of RV outflow tract, subtricuspid RV, and interventricular septum. Late potentials were never recorded.

The patient-level analysis of LVAs showed larger low-voltage regions in unipolar and bipolar maps (UV ≤ 5.5 mV: 32.3 ± 6.1 cm^2 vs 12.4 ± 9.6 cm^2 [$P < 0.001$]; BV ≤ 1.5 mV: 18.0 ± 5.5 cm^2 vs 8.2 ± 7.5 cm^2 [$P = 0.012$]), as

Table 3. Associations of electroanatomic features at sites of endomyocardial biopsy with amyloid and replacement-type fibrosis burdens at histopathologic analysis

EGM feature	Coefficient	Standard error	*P* value
Association of electrogram features and amyloid burden			
Unipolar EGM amplitude	−3.27	0.94	0.001*
Bipolar EGM amplitude	−2.96	1.28	0.025*
EGM duration	0.08	0.17	0.657
No. of EGM peaks	7.10	5.43	0.198
Association of EGM features and replacement-type fibrosis burden			
Bipolar EGM amplitude	−0.57	0.23	0.017*
EGM duration	0.07	0.03	0.033*
Unipolar EGM amplitude	−0.34	0.19	0.071
No. of EGM peaks	1.1605	1.520.99	0.250

EGM, electrogram.
* $P < 0.05$.

well as larger DSA (BV < 0.5 mV: 5.8 cm^2 [Q1-Q3 3.2-8.0 cm^2] vs 2.0 cm^2 [Q1-Q3 1.1-3.2 cm^2]), in AL compared with ATTR CA (Fig. 1). At area under the receiver operating characteristic curve (AUC) analysis, unipolar LVA allowed highest discrimination (AUC_{UniLVA} 0.94 [95% confidence interval [CI] 0.83-1.00]), followed by bipolar LVA (AUC_{BipLVA} 0.88 [95% CI 0.70-1.00]) and DSA (AUC_{DSA} 0.82 [95% CI 0.60-1.00]) (Fig. 1) for the distinction of AL and ATTR CA (Fig. 1). The cutoffs in the extemts of unipolar LVA, bipolar LVA, and DSA that that best distinguished patients with AL CA from patients with ATTR CA were, respectively, 25.9 cm^2 (sensitivity 100%, specificity 89%, accuracy 93%), 12.9 cm^2 (sensitivity 83%, specificity 89%, accuracy 87%), and 5.5 cm^2 (sensitivity 50%, specificity 89%, accuracy 73%). The results of the analysis on the association of pooled EGM amplitude with CA type are reported in Supplemental Appendix S2 and Supplemental Figure S1.

EGM analysis at EMB sites

A total of 57 EMB samples were retrieved, all of which were collected from the interventricular septum. No patient experienced complications requiring invasive urgent management, and we observed no pericardial effusion or cardiac tamponade, new atrioventricular/bundle branch block, or worsening of tricuspid regurgitation after EVM and EMB.

A final biopsy-proven diagnosis of AL or ATTR CA was formulated in 6 (40%) and 9 (60%) patients, respectively. ATTR CA was diagnosed in 7 patients with positive ^{99m}Tc-HDP scintigraphy and positive serum immunofixation, as well as in the 2 patients with clinical/imaging suspicion of hypertrophic cardiomyopathy. Of the 6 patients with a biopsy-proven diagnosis of AL-CA, 1 had grade 2 ^{99m}Tc-HDP scintigraphy and 1 was an Afro-Caribbean woman with family history of ATTR CA, harbouring aheterozygous p.VAL142Ile mutation of the TTR gene.

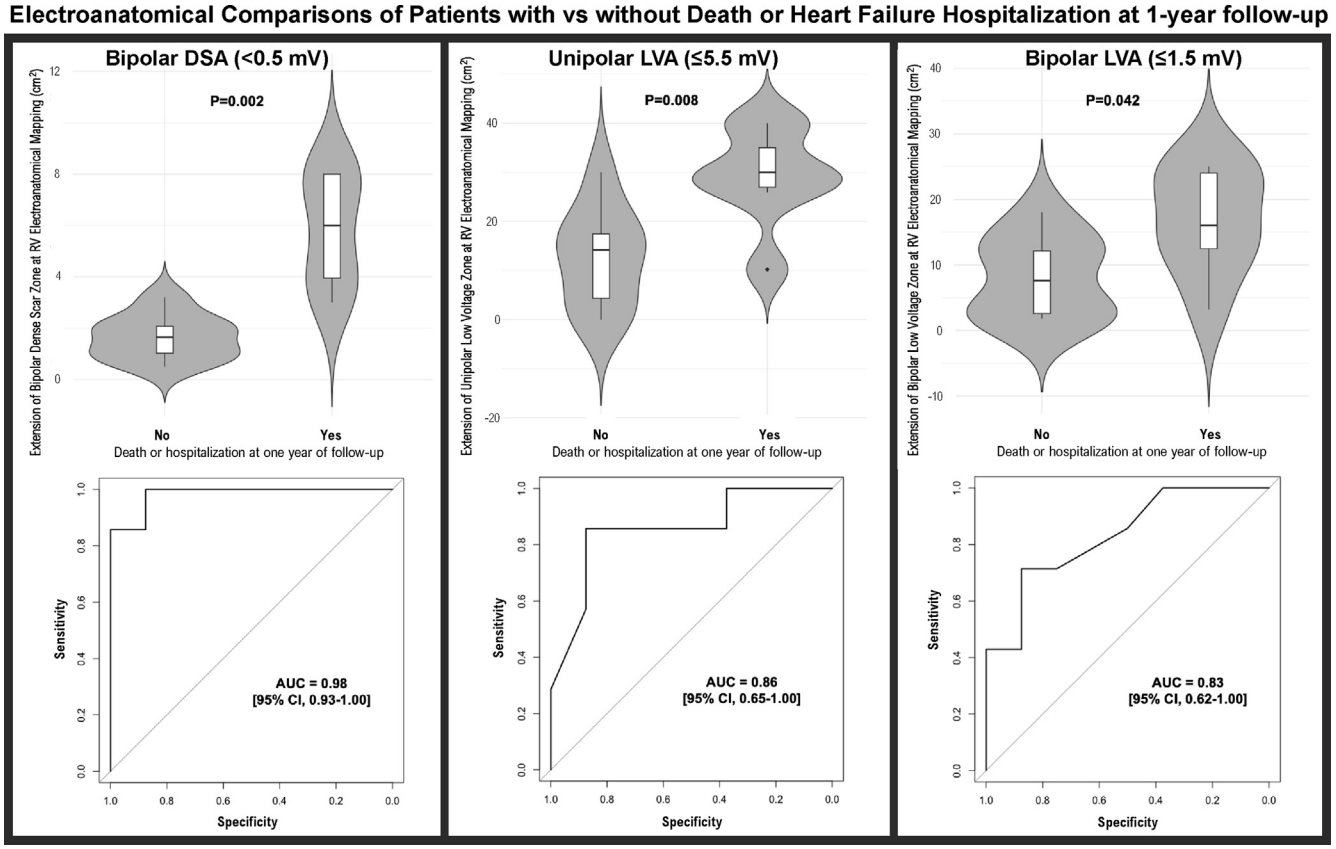

Figure 3. Electroanatomic comparisons between patients with vs without primary outcome events. AL, immunoglobulin light chain–related; AUC, area under the receiver operatic characteristic curve; ATTR, transthyretin-related; CA, cardiac amyloidosis; CI, confidence interval; DSA, dense scar area; EMB, endomyocardial biopsy; LVA, low-voltage area.

Table 4. Univariable and multivariable predictors of primary outcome events at logistic regression analysis

Variable	Univariable analysis			Multivariable analysis		
	OR	95% CI	*P* value	OR	95% CI	*P* value
Age, y†	0.92	0.80-1.01	0.080			
Female sex	2.02	0.27-17.23	0.491			
Biopsy-proven type of CA						
ATTR CA (vs AL CA)	0.09	0.01-0.76	0.026*	2.85	0.05-217.56	0.681
NYHA functional class III (vs II)†	3.42	0.47-23.40	0.231			
BMI, kg/m^2†	0.89	0.66-1.17	0.423			
COPD	0.60	0.05-5.87	0.660			
TTR variant	1.15	0.08-17.05	0.911			
^{99m}Tc-HDP scintigraphy grade						
2 (vs 0)	0.15	0.01-1.40	0.099			
3 (vs 0)	0.20	0.01-2.78	0.233			
GFR, mL/min†	1.01	0.97-1.07	0.570			
NT-proBNP, ng/L†	1.00	0.99-1.00	0.055			
Disease stage						
2 (vs 1)	2.20	0.13-40.49	0.569			
3 (vs 1)	13.44	1.31-262.74	0.027*	9.01	0.05-352.16	0.341
History of atrial fibrillation	1.29	0.07-3.38	0.473			
Nonsustained ventricular tachycardia	3.89	0.46-50.89	0.217			
ECG data						
Low QRS voltage	0.85	0.10-7.33	0.875			
Limb QRS score, mV†	0.85	0.66-1.01	0.058			
Precordial QRS score, mV†	0.96	0.89-1.02	0.212			
Total QRS score, mV†	0.96	0.90-1.01	0.126			
Atrial fibrillation	0.36	0.03-3.06	0.357			
PR interval, ms†	0.97	0.90-1.01	0.109			
Any intraventricular conduction disturbance	6.81	0.86-89.80	0.070			
LBBB	0.60	0.05-5.87	0.660			
RBBB	7.73	0.50-1148.84	0.153			
LAFB	2.27	0.23-30.51	0.478			
LPFB	7.73	0.50-1148.84	0.153			
T-wave inversion	3.34	0.47-29.40	0.231			
Imaging data‡						
Maximal septal thickness, mm†	0.75	0.43-1.10	0.152			
Posterior wall thickness, mm†	0.96	0.62-1.48	0.854			
LVEDD, mm†	0.97	0.79-1.19	0.776			
iLVEDV, mL/m^2†	0.98	0.88-1.09	0.733			
iLAV, mL/m^2†	1.02	0.94-1.13	0.614			
LVEF, %†	0.93	0.82-1.01	0.089			
E/e′†	1.18	0.97-1.56	0.135			
RVD1, mm†	0.99	0.79-1.22	0.919			
Right atrial area, cm^2†	1.01	0.88-1.19	0.803			
TAPSE, mm†	0.77	0.44-1.10	0.168			
sPAP, mm Hg†	1.01	0.72-1.01	0.890			
CMR performed	1.85	0.30-11.28	0.504			
Electrophysiologic/electroanatomic data						
AH interval, ms†	0.95	0.90-1.01	0.080			
HV interval, ms†	1.03	0.96-1.14	0.407			
PVS performed	2.27	0.23-30.51	0.478			
RV mapped area, cm^2†	1.01	0.98-1.05	0.529			
Bipolar low-voltage zone (≤ 1.5 mV), cm^2†	1.15	1.003-1.391	0.045*	0.73	0.29-1.19	0.220
Bipolar dense scar (< 0.5 mV), cm^2†	5.25	1.39-566.61	< 0.001*	2.40	1.05-11.70	0.037*
Unipolar low-voltage zone (≤ 5.5 mV), cm^2†	1.13	1.02-1.33	0.012*	1.16	0.82-2.02	0.384
Endomyocardial biopsy data						
Average amyloid percentage†	0.99	0.92-1.06	0.753			
Average replacement-type fibrosis percentage†	0.86	0.53-1.29	0.470			
Medical treatments						
Tafamidis	0.29	0.03-2.02	0.214			
Loop diuretics	9.55	0.70-1388.65	0.095			
Mineralocorticoid receptor antagonists	5.72	0.78-56.57	0.087			
Thiazide/thiazide-like diuretics	0.33	0.002-7.34	0.496			
SGLT2 inhibitors	3.92	0.18-612-55	0.392			
Oral anticoagulants	0.45	0.05-3.20	0.418			
Antiplatelets	1.18	0.14-10.33	0.875			
Statins	0.16	0.01-1.27	0.082			
Beta-blockers	0.45	0.05-3.20	0.431			
Amiodarone	3.92	0.18-612.55	0.392			
Angiotensin-converting enzyme inhibitors	0.17	0.01-2.67	0.226			

Table 4. Continued.

Variable	Univariable analysis			Multivariable analysis		
	OR	95% CI	*P* value	OR	95% CI	*P* value
Angiotensin receptor blockers	0.17	0.01-2.67	0.226			

AL, immunoglobulin light chain–related; ATTR, transthyretin-related; BMI, body mass index; CA, cardiac amyloidosis; CMR, cardiac magnetic resonance imaging; COPD, chronic obstructive pulmonary disease; GFR, glomerular filtration rate; iLAV, indexed left atrial volume; iLVEDV, indexed left ventricular end-diastolic volume; LAFB, left anterior fascicular block; LBBB, left bundle branch block; LGE, late gadolinium enhancement; LPFB, left posterior fascicular block; LVEDD, left ventricular end-diastolic diameter; LVEF, left ventricular ejection fraction; NT-proBNP, N-terminal pro–B-type natriuretic peptide; NYHA, New York Heart Association; RBBB, right bundle branch block; RV, right ventricular; RVD1, basal right ventricular diameter; SGLT2, sodium-glucose cotransporter 2; sPAP, systolic pulmonary artery pressure; TAPSE, tricuspid annular plane systolic excursion; ^{99m}Tc-HDP, hydroxydiphosphonate technetium; TTR, transthyretin.

* $P < 0.05$.

† Per unit increase.

‡ For wall thickness, volumes, and ejection fraction, cardiac magnetic resonance data were reported, when available.

At histopathologic analysis, amyloid covered a median 22% (Q1-Q3 9%-36%) of samples, while replacement-type fibrosis was scarce (median 2% [Q1-Q3 0-3%]). Of note, low UV and BV were recorded in 14 (25%) and 13 (23%) sampling sites, respectively. We observed a negative and significant correlation between UV at sampling site and amyloid percentage at that site ($P = 0.001$) (Fig. 2; Table 3), as well as between BV and both amyloid percentage ($P = 0.025$) (Table 3) and fibrosis percentage ($P = 0.017$) (Fig. 2; Table 3). In addition, EGM duration was associated with the amount of replacement fibrosis ($P = 0.033$) (Table 3). On the other hand, the number of EGM peaks at EMB sites were not significantly related to the percentages of amyloid or replacement-type fibrosis (Table 3). The results of the mixed-effects models, in which the patient was accounted for as an independent random effect, are reported as sensitivity analyses in Supplemental Table S2. The unipolar and bipolar voltage cutoffs that best identified regions with > 15% amyloid tissue infiltration according to the Youden index were, respectively, 5.5 mV (sensitivity 100%, specificity 31%, accuracy 57%), and 1.48 mV (sensitivity 88%, specificity 26%, accuracy 65%).

Clinical outcomes

By the end of 1 year of follow-up, 7 patients (47%) had a primary outcome event. Notably, 3 patients (27%) died, among them a sudden and unexplained death in a 41-year-old male patient with AL CA and 40% left ventricular ejection fraction. The other 2 deaths were due to pulseless electrical activity cardiac arrest and refractory heart failure. Furthermore, 6 patients (40%) required hospitalisation for heart failure worsening. Patients with a primary outcome event were more commonly affected by AL CA and had lower left ventricular ejection fraction, higher NT-proBNP levels, and higher disease stage (Supplemental Table S1).

We found larger bipolar DSA (6.1 ± 2.3 cm^2 vs 1.8 ± 0.7 cm^2; $P = 0.005$), and larger unipolar and bipolar LVAs (unipolar LVA 29.2 ± 10.1 cm^2 vs 12.7 ± 10.2 cm^2 [$P = 0.008$]; bipolar LVA 16.7 ± 8.1 cm^2 vs 8.1 ± 6.3 cm^2 [$P = 0.042$]) (Fig. 3; Table 4) in patients experiencing a primary outcome event compared with patients with uneventful follow-up in the patient-level analysis. Receiver operating characteristic curves are shown in Figure 3. The optimal cutoffs that best predicted the occurrence of a primary outcome event according to the Youden index were a bipolar DSA > 3 cm^2 or > 2% of the mapped RV area (sensitivity 100%, specificity 88%, accuracy 93%), a unipolar LVA > 25.9 cm^2 or > 14% of the mapped RV area (sensitivity 86%, specificity 88%, accuracy 87%), and a bipolar LVA > 12.9 cm^2 or > 8% of the mapped RV area (sensitivity 71%, specificity 88%, accuracy 80%).

In addition, in logistic regression analysis, the extents of bipolar LVA and DSA, as well as of unipolar LVA, were associated with higher odds of primary outcome events at univariable analysis; the extent of DSA retained a significant association in multivariable analysis (OR 2.40, 95% CI 1.05-11.70; $P = 0.037$), after adjusting for the type of CA, disease stage, and unipolar/bipolar LVA (Table 4, Fig. 4).

The results of the analysis of the association between pooled EGM amplitude and primary outcome events, as well as the analysis of electroanatomic predictors of death are reported in Supplemental Appendix S2 and Supplemental Figure S2.

Discussion

This work presents the first systematic assessment of electroanatomic features of CA. Our results suggest several main messages for clinicians, as follows.

1) EMB can be useful when other tests fail to diagnose and type CA, which is required for the prescription of effective disease-modifying therapies.[1]
2) Patients with advanced CA have a modest yet diffuse reduction of BV and UV; electroanatomic dense scar according to conventional cutoffs is uncommon, covering a median of 3% of the mapped RV area.
3) Compared with ATTR CA, we found larger unipolar/bipolar LVAs, wider bipolar DSAs, and lower average EGM peak-to-peak amplitudes in AL CA, suggesting that electroanatomic data might be sensitive to the type of CA.
4) EGM peak-to-peak amplitude is related to the percentage of amyloid tissue in EMB samples, representing a quantitative marker of amyloid burden, while bipolar EGM peak-to-peak amplitude is also associated with the extent of replacement-type fibrosis.
5) We observed an independent association between larger bipolar DSAs and worse clinical outcomes, suggesting that EVM may have prognostic value.

Diagnostic role of EMB in CA

A precise diagnosis of CA type has major prognostic and therapeutic implications. If left untreated, AL CA has a

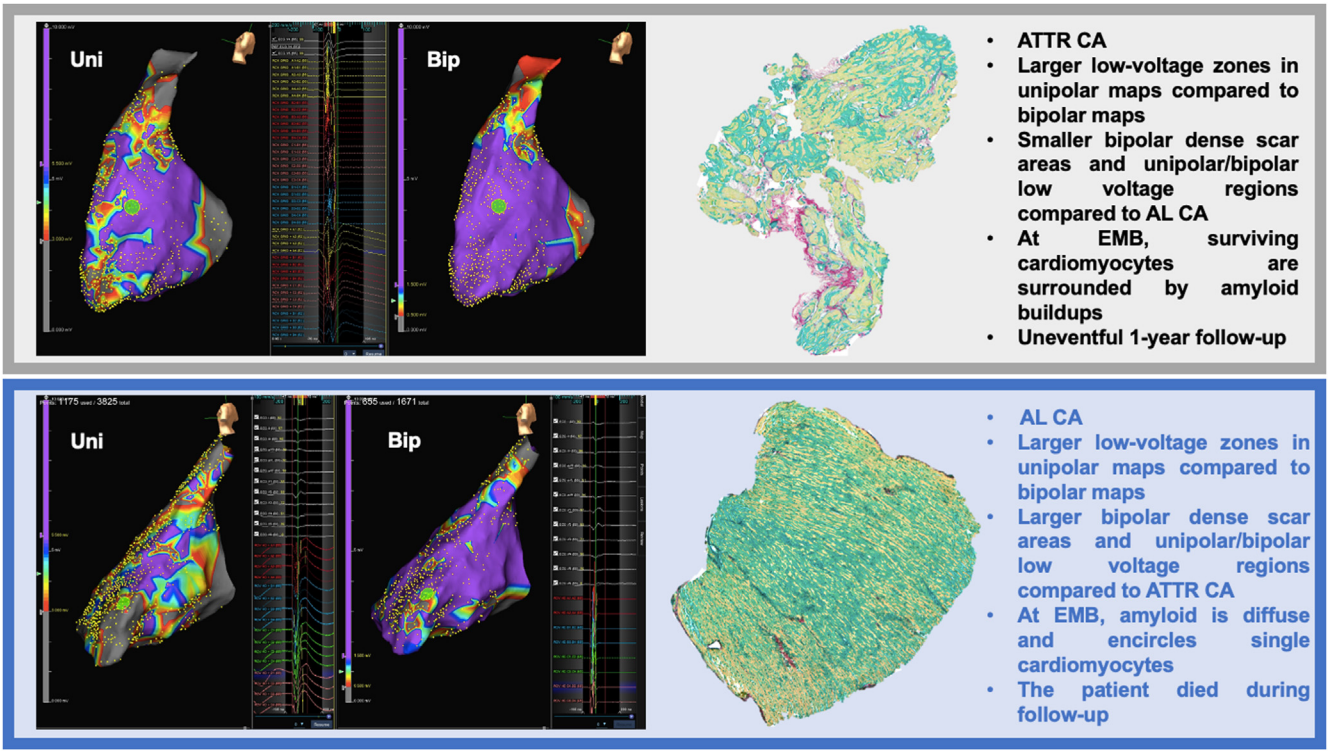

Figure 4. Examples of patients with cardiac amyloidosis (CA), different electroanatomic substrate, and divergent outcomes. In endomyocardial biopsies (Sulfated Alcian Blue stain; **scale bar** = 100 μm), amyloid is coloured **green** and cardiomyocytes are coloured **yellow**; note that fibrous tissue (**red**) is scarce. AL, immunoglobulin light chain–related; ATTR, transthyretin-related; Bip, bipolar voltage mapping; EMB, endomyocardial biopsy; Uni, unipolar voltage mapping.

prognosis of < 6 months,[21] whereas ATTR CA is associated with a median survival of 3-5 years after diagnosis.[22] Furthermore, a definite diagnosis of CA type (AL vs ATTR) is crucial, because treatment approaches are completely different.[1,4] Most patients included in the present study had monoclonal proteins, thus requiring histologic confirmation to diagnose and/or subtype CA according to international recommendations.[1] EMB with the use of EVM and ICE allowed a diagnosis of CA type in all cases, while also proving to be safe in this clinical context. Consistent with what was previously reported by us in other clinical contexts[9-13,23] as well as by other groups,[6,7] EMB proved to be safe, with no major complications. We may speculate that tissue sampling of the thickened interventricular septum with verification of proper bioptome positioning with ICE and avoiding mechanical injuries to the conduction system with EVM may optimally balance diagnostic accuracy and safety in patients with CA.

Electroanatomic features of CA

To the best of our knowledge, this is the first report on the use of high-density EVM in patients with CA. Although there was a very high prevalence of low QRS voltages on ECG, the average peak-to-peak EGM amplitudes were around the lower limit of normal, with limited LVAs commonly affecting more than 1 anatomic region of the RV, and rare bipolar DSAs. In this context, we found a significant association of UV and BV with amyloid burden at EMB. The rarity of very-low-voltage EGMs may be explained by the low amount of replacement-type fibrosis in our cohort, by the concomitant preservation of cardiac myocytes, and by the small dimensions of mapping electrodes.[24,25] In a study using whole human heart histology validation, Glashan et al. reported that both BV and UV are linearly associated with wall thickness.[26] As a result of amyloid infiltration, patients in our cohort had markedly increased wall thicknesses (median interventricular septal thickness 18 mm). Therefore, we may conclude that in CA, UV and BV are close to the lower limit of normal yet disproportionately low compared with the degree of parietal hypertrophy, in accordance with what is known for the relationship between ECG voltage and wall thickness in CA.[27] Furthermore, we noted larger LVA and DSA in AL compared with ATTR CA. Although this finding may be explained by a difference in amyloid burden (and consequently in the amount surviving myocytes), we cannot exclude that amyloid fibrils from different precursor proteins have different electrophysiologic properties, as suggested by recent evidence from ECG imaging studies of CA,[28] with a possible role of the well known direct cytotoxic effect of AL amyloid fibrils.[1]

Clinical value of EVM in CA

Several validated clinical tools using biomarkers allow prognosis estimation in CA,[1] and cardiac imaging may refine the prognostication process.[29] CMR-derived extracellular volume (ECV), currently regarded as a preferred noninvasive measure of amyloid burden, has emerged as an important

marker of disease severity and predictor of clinical outcomes.[29,30] However, no histopathologic validation was systematically performed for extracellular volume in CA, and this parameter appears to be sensitive to several heterogeneous histopathologic processes, including amyloid deposition and intra-/extracellular edema.[29,30] In our present study, we found that BV and UV are associated with the extent of amyloid deposition at EMB, and that BV is also associated with EMB-proven replacement-type fibrosis burden. Consistently, we could detect an independent association of larger bipolar DSAs with adverse clinical outcomes. Therefore, there might be a prognostic rationale for performing EVM in combination with EMB among patients with CA needing histopathologic confirmation of diagnosis.

Limitations and future perspectives

Several limitations should be acknowledged. First, this was a small single-centre study, which limits the statistical power of observations and the generalisability of results. Second, only the RV chamber was mapped. However, CA is usually characterised by diffuse tissue infiltration, and diffuse biventricular late gadolinium enhancement was demonstrated among patients who underwent CMR in our cohort. Third, owing to the poor spatial resolution of late gadolinium enhancement in the RV and the unavailability of T mapping at our institution, we could not systematically assess the regional correlation between CMR tissue characterisation findings and EVM. Fourth, our data did not allow speculations concerning the risk of life-threatening ventricular arrhythmias and sudden cardiac death in CA, and the possible role of PVS and EVM in this setting should be the subject of further investigations.

Conclusion

EMB with use of EVM and ICE allowed us to confirm the diagnosis of CA and to identify the amyloid precursor protein in each case, with no major adverse events. CA appeared to have a distinct electroanatomic substrate, characterised by EGM amplitudes around the lower limit of normal yet of disproportionately low amplitude compared with the increased wall thickness. We found evidence that BV and UV may be quantitative markers of amyloid burden, and that the extent of bipolar DSA may be an important predictor of risk of death or heart failure hospitalisation.

Acknowledgements

We thank Valentina la Piscopia, BE, and Barbara Bondavalli, BE, for assistance in data extraction from the electroanatomic mapping system.

Ethics Statement

The study was approved by the Institutional Review Board.

Patient Consent

The authors confirm that patient consent forms have been obtained for this article.

Funding Sources

The authors have no funding sources to declare.

Disclosures

Dr Casella has received speaker honoraria from Biosense Webster. Dr Vagnarelli has received speaker honoraria from Pfizer. Dr Lofiego has received speaker honoraria from Pfizer. Dr Natale is a consultant for Biosense Webster, Stereotaxis, and Abbott Medical, and has received speaker honoraria/travel from Medtronic, Atricure, Biotronik, and Janssen. Dr Dello Russo is a consultant for Abbott Medical. The other authors have no conflicts of interest to disclose.

References

1. Kittleson MM, Ruberg FL, Ambardekar AV, et al. 2023 ACC expert consensus decision pathway on comprehensive multidisciplinary care for the patient with cardiac amyloidosis: a report of the American College of Cardiology Solution Set Oversight Committee. J Am Coll Cardiol 2023;81:1076-126.
2. González-López E, Gallego-Delgado M, Guzzo-Merello G, et al. Wild-type transthyretin amyloidosis as a cause of heart failure with preserved ejection fraction. Eur Heart J 2015;36:2585-94.
3. Giancaterino S, Urey MA, Darden D, Hsu JC. Management of arrhythmias in cardiac amyloidosis. JACC Clin Electrophysiol 2020;6:351-61.
4. Ciliberti G, Urbinati A, Barbarossa A, et al. Compassionate drug use for patients with transthyretin amyloid cardiomyopathy. J Cardiovasc Med (Hagerstown) 2021;22:792-4.
5. Maleszewski JJ. Cardiac amyloidosis: pathology, nomenclature, and typing. Cardiovasc Pathol 2015;24:343-50.
6. Hahn VS, Yanek LR, Vaishnav J, et al. Endomyocardial biopsy characterization of heart failure with preserved ejection fraction and prevalence of cardiac amyloidosis. JACC Heart Fail 2020;8:712-24.
7. Pucci A, Aimo A, Musetti V, et al. Amyloid deposits and fibrosis on left ventricular endomyocardial biopsy correlate with extracellular volume in cardiac amyloidosis. J Am Heart Assoc 2021;10:e020358.
8. Seferović PM, Tsutsui H, Mcnamara DM, et al. Heart Failure Association, Heart Failure Society of America, and Japanese Heart Failure Society position statement on endomyocardial biopsy. J Card Fail 2021;27:727-43.
9. Casella M, Pizzamiglio F, Dello Russo A, et al. Feasibility of combined unipolar and bipolar voltage maps to improve sensitivity of endomyocardial biopsy. Circ Arrhythm Electrophysiol 2015;8:625-32.
10. Casella M, Dello Russo A, Bergonti M, et al. Diagnostic yield of electroanatomic voltage mapping in guiding endomyocardial biopsies. Circulation 2020;142:1249-60.
11. Dello Russo A, Compagnucci P, Casella M, et al. Ventricular arrhythmias in athletes: role of a comprehensive diagnostic workup. Heart Rhythm 2022;19:90-9.
12. Casella M, Bergonti M, Dello Russo A, et al. Endomyocardial biopsy: the forgotten piece in the arrhythmogenic cardiomyopathy puzzle. J Am Heart Assoc 2021;10:e021370.
13. Casella M, Gasperetti A, Compagnucci P, et al. Different phases of disease in lymphocytic myocarditis: clinical and electrophysiological characteristics. JACC Clin Electrophysiol 2023;9:314-26.

14. Pelargonio G, Pinnacchio G, Narducci ML, et al. Long-term arrhythmic risk assessment in biopsy-proven myocarditis. JACC Clin Electrophysiol 2020;6:574-82.

15. Perugini E, Guidalotti PL, Salvi F, et al. Noninvasive etiologic diagnosis of cardiac amyloidosis using ^{99m}Tc-3,3-diphosphono-1,2-propanodicarboxylic acid scintigraphy. J Am Coll Cardiol 2005;46:1076-84.

16. Bergonti M, Casella M, Compagnucci P, Russo AD, Tondo C. Electroanatomic mapping system and intracardiac-echo to guide endomyocardial biopsy. Card Electrophysiol Clin 2021;13:381-92.

17. Venlet J, Piers SR, Jongbloed JD, et al. Isolated subepicardial right ventricular outflow tract scar in athletes with ventricular tachycardia. J Am Coll Cardiol 2017;69:497-507.

18. Barbhaiya CR, Kumar S, Baldinger SH, et al. Electrophysiologic assessment of conduction abnormalities and atrial arrhythmias associated with amyloid cardiomyopathy. Heart Rhythm 2016;13:383-90.

19. Gasperetti A, Carrick RT, Costa S, et al. Programmed ventricular stimulation as an additional primary prevention risk stratification tool in arrhythmogenic right ventricular cardiomyopathy: a multinational study. Circulation 2022;146:1434-43.

20. Firth D. Bias reduction of maximum likelihood estimates. Biometrika 1995;82:667.

21. Tahir UA, Doros G, Kim JS, et al. Predictors of mortality in light chain cardiac amyloidosis with heart failure. Sci Rep 2019;9:8552.

22. Lane T, Fontana M, Martinez-Naharro A, et al. Natural history, quality of life, and outcome in cardiac transthyretin amyloidosis. Circulation 2019;140:16-26.

23. Peretto G, Casella M, Merlo M, et al. Inflammation on endomyocardial biopsy predicts risk of MACE in undefined left ventricular arrhythmogenic cardiomyopathy. JACC Clin Electrophysiol 2023;9(7 Pt 1):951-61.

24. Berte B, Zeppenfeld K, Tung R. Impact of micro-, mini- and multi-electrode mapping on ventricular substrate characterisation. Arrhythm Electrophysiol Rev 2020;9:128-35.

25. Dello Russo A, Compagnucci P, Bergonti M, et al. Microelectrode voltage mapping for substrate assessment in catheter ablation of ventricular tachycardia: a dual-center experience. J Cardiovasc Electrophysiol 2023;34:1216-27.

26. Glashan CA, Androulakis AFA, Tao Q, et al. Whole human heart histology to validate electroanatomical voltage mapping in patients with nonischaemic cardiomyopathy and ventricular tachycardia. Eur Heart J 2018;39:2867-75.

27. Carroll JD, Gaasch WH, mcadam KP. Amyloid cardiomyopathy: characterization by a distinctive voltage/mass relation. Am J Cardiol 1982;49:9-13.

28. Orini M, Graham AJ, Martinez-Naharro A, et al. Noninvasive mapping of the electrophysiological substrate in cardiac amyloidosis and its relationship to structural abnormalities. J Am Heart Assoc 2019;8:e012097.

29. Knight DS, Zumbo G, Barcella W, et al. Cardiac structural and functional consequences of amyloid deposition by cardiac magnetic resonance and echocardiography and their prognostic roles. JACC Cardiovasc Imaging 2019;12:823-33.

30. Martinez-Naharro A, Kotecha T, Norrington K, et al. Native T1 and extracellular volume in transthyretin amyloidosis. JACC Cardiovasc Imaging 2019;12:810-9.

Supplementary Material

To access the supplementary material accompanying this article, visit the online version of the *Canadian Journal of Cardiology* at www.onlinecjc.ca and at https://doi.org/10.1016/j.cjca.2023.10.022.